Fatigue Crack Sizing of Skew and Thumbnail Cracks Using an AC Potential Drop System

R.B. Tait* and D. Bright**

* Department of Mechanical Engineering, University of Cape Town, Rondebosch, Cape Town, 7701, South Africa. btait@eng.uct.ac.za
** Department of Electrical Engineering, University of Cape Town, Rondebosch, Cape Town, 7701, South Africa, mwdoz@mweb.co.za

ABSTRACT. *An ACPD method has been developed as an NDT technique that can accurately characterize surface breaking fatigue cracks in metal specimens. Single fatigue cracks that were initiated and propagated in different specimens were considered. The ACPD system was sensitive (capable of detecting fatigue crack increments as small as 45 microns) and able to discriminate skew cracks from 15 to 90 degrees, as well as fatigue cracks of variable aspect ratio. Finally, the effects, on ACPD detectability, of stress across the crack, where electrical crack wake closure may play a role, was also considered, together with the potential for industrial application.*

INTRODUCTION

Background

The development of fatigue cracks in industrial components is still, unfortunately, not a rare occurrence, and it is important that the structural integrity of all the systems and equipment being utilized by the facility is assured. Any flaws, particularly fatigue cracks present in a structure, can be assessed by a "fitness-for-purpose" Fracture Mechanics approach, which requires that all the defects be below a maximum specified size in order for the structure to function at the required level of safety for the necessary length of time. The fracture mechanics perspective assesses the interrelationship between the size of an inherent flaw, a, in a structure, in conjunction with the stresses the system sustains, σ, to a local stress intensity, K. When K exceeds the local material's resistance to cracking, or its "fracture toughness", K_{IC}, fast, brittle failure is imminent, i.e.

$$Y\sigma\sqrt{(\pi a)} = K \qquad \text{(stress intensity)} \tag{1}$$

and, when $K > K_{IC}$, failure occurs.

In addition, equation (1) also includes a compliance function Y, which is dimensionless and takes into account the shape of the flaw as well as the relative dimensions of the component

in which the flaw is located. From this expression, it is clear that the flaw size is critical in determining whether a material is susceptible to failure under an applied load. This interrelationship between the stress, flaw size and toughness is sometimes referred to as the "triangle of integrity", and is applicable even when tougher materials are employed. In this case it is appropriate to use COD or J integral toughness characterizations and an EPFM approach, rather than linear elastic (brittle) formulations.

To determine the structural integrity of an engineering system precisely using equation (1) or its plastic equivalent, not only must the depth of the flaw, *a*, be established, but the crack profile must also be obtained in order to assess the extent of the crack, as shown in Fig. 1. That is, the aspect ratio (crack depth to crack surface length, *a / 2c*) must be obtained, thus enabling determination of the *Y* function, and facilitating the "fitness-for-purpose" fracture mechanics assessment.

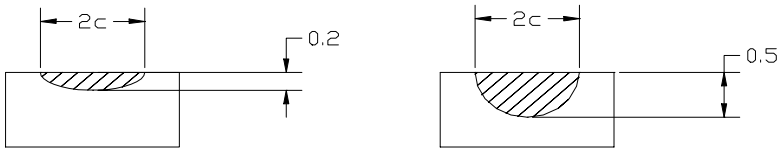

Figure 1. Thumbnail cracks with identical surface lengths (2c), but different aspect ratios.

Many NDT procedures do not necessarily give an accurate characterisation of the crack size in a material [1-4]. Optical and surface methods such as dye penetrant and magnetic particle inspection (MPI), although convenient for crack detection, do not provide crack depth readings. X-Ray methods can detect globular type flaws, but are not suitable for tight fatigue cracks. Eddy current testing is reliable for surface crack detection, but is not accurate in sizing such defects. Ultrasonic pulse-echo (PE) approaches, although widely used, have a relatively large sizing error (typically ± 5mm) and even time-of–flight diffraction (TOFD), although a lot more accurate (± 0.4mm), is very labour intensive as the testing procedure can be tedious, and accuracy can only be provided at relatively great expense. The potential drop (PD) technique, however, has been used previously as a research tool in flaw characterisation, and has achieved good accuracy [5-16]. The present work described in this paper discusses the NDT development of an ACPD system for flaw sizing of variously shaped and oriented surface breaking fatigue cracks.

Theory

The principle of the ACPD method lies in Ohm's Law, where a conductor carrying a current will exhibit a resistance. This resistance is proportional to the potential drop (PD) measured across the conductor, and is a function of specimen material, environmental

effects (e.g. temperature), and length of the current path. Thus, if the current path length is altered by a fatigue crack, there will be a proportional increase in the potential drop.

Studies conducted have revealed that the output of the ACPD system is dependent on other factors, including: input current magnitude and frequency, loading history and material plasticity, crack closure, electromagnetic effects, edge effects, temperature and voltage probe configuration [5-16]. In order to develop an accurate crack characterization system, all of the features of this technique must be examined.

EXPERIMENTAL DETAILS

In the present case, PD characteristics were investigated by passing a current through various conducting metal specimens in which cracks could be introduced, both manually and by fatigue, and measuring the PD across any such defect, and in the nearby vicinity. The associated equipment, discussed below, facilitated this procedure.

In this study, a dual voltage probe system was adopted, which compared the voltage across the crack to some reference voltage measured away from the crack. This system eliminates thermoelectric and other temperature effects, and maintains the positions of the probe leads constant, thereby eliminating inductive effects. It is also important to note that the loading applied to the specimens was sufficiently low that there was only a small plastic region in the specimens, and the rate of crack propagation was held constant to maintain this small but constant plastic zone size. Thus, any voltage associated with localised work hardening could therefore be ignored.

Experimental System

A variac and a transformer, connected to mains, supplied the input current of 0.5A at 50Hz. The voltage signals from the specimen passed through an electronic circuit that amplified, filtered and converted the noisy AC signals into clean DC voltages. The output of the circuit was measured by an HP34401A digital multimeter, which was controlled by a PC running different programs written in HP Vee. For every measurement made by the multimeter, ten voltage readings were taken and analysed. As the mains signal is notoriously noisy and unstable, a dual voltage probe system was adopted, so that a reference voltage could be provided to negate the effects of the unpredictable signal. The 50Hz signal resulted in a skin depth of 0.8mm in steel, and caused less voltage to be induced in the probe leads.

Electronic Measurement System

The electronic system presented in this paper evolved as needs for a more accurate and sensitive device was required, and was considered in three phases. In Phase I the ACPD system was based on a synchronous detection system, but the voltage measured across the crack was divided by the reference voltage, and not multiplied as in a regular synchronous detection system, yielding a so called PD $_{ratio.}$ This was extended in Phase II using a

complete dual channel system, where the AC voltage signals across the crack and at some remote reference point, were separately amplified, filtered and converted to DC. This system provided a more accurate PD ratio.

The final step in the development evolution of the PD system, Phase III, was the introduction of an instrumentation amplifier at the output of the dual channel circuit, to provide an accurate differential signal by comparing the crack voltage to the reference voltage. The output signal V_{dc} was a direct indication of the difference in the distance the current traveled between the pairs of probes only, and thus provided a direct measure of the resistance which could be related to the depth of the crack.

Material and Specimen Geometry

Two different materials, mild steel and 7075 aluminium, were used for the preparation of bend type specimens, of various sizes. For through thickness cracking, specimens had a thickness range of 2 to 8mm, which included specimens for so called "skew cracks".

The final steel specimen type (Fig. 2) was a thumbnail ribbed bending (TRB) specimen of basic dimensions 240 by 50 by 20mm, which included a machined rib of width either 5 or 15mm [17]. This ribbed specimen was pre-fatigued until a crack propagated through the rib and into the body of the specimen. The rib was then machined off to provide a smooth surface for NDT inspection, but with the specimen containing a sharp, tight fatigue crack, with variable and controllable aspect ratio.

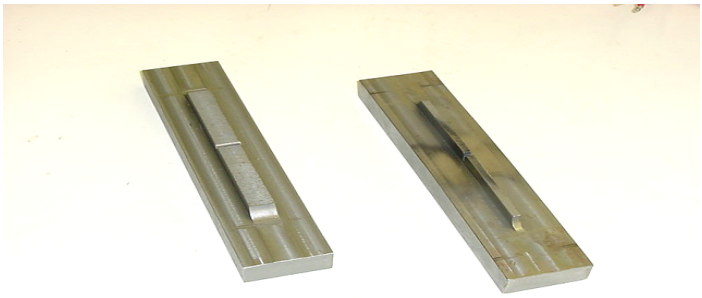

Figure 2. The TRB specimens, displaying the different rib widths. The specimen on the left has a rib of 15mm width, and the specimen on the right has a rib 5mm thick. Fatigue cracks were grown through the rib, which was then machined off leaving a tight fatigue crack in the bulk specimen.

RESULTS AND DISCUSSION

Sensitivity Test Results

Tests to evaluate the sensitivity of the ACPD system to fatigue crack sizing were conducted using the Phase III system and the results displayed in Fig. 3. For crack depths smaller than

the skin depth, the ACPD device is not very sensitive, as the current can merely flow around the crack without much change in the current path. However, once the crack extends past the skin depth, the sensitivity of the system to an increase in the crack depth was enhanced. From the results, a 0.1 mm change in crack length, gives an average PD ratio change of 10 mV. The maximum standard deviation of the readings was determined experimentally to be $2*10^{-3}$, therefore, the sensitivity of the device *S*, in terms of detectable crack length increment, can be calculated to be

$$S = 0.1/(10/(2*2)) = 40\ \mu m$$

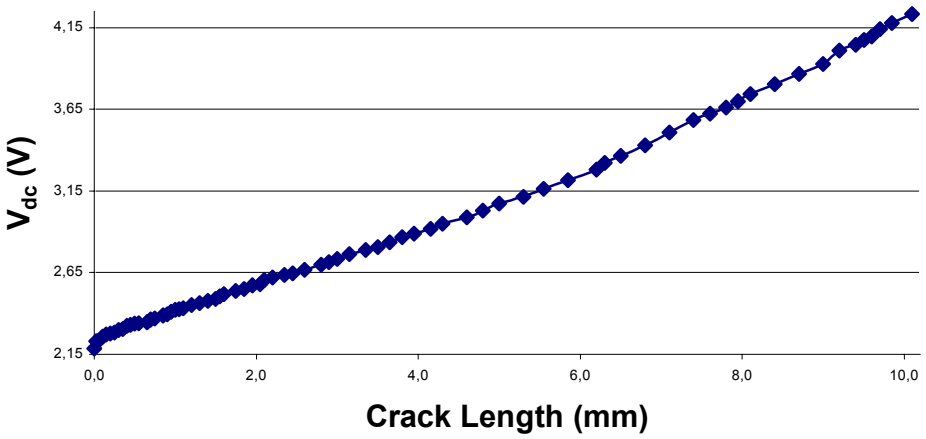

Figure 3. Graph of V_{dc} vs Fatigue Crack Length for Phase III.

Skew Crack Results

The PD results for the Phase I system are given below in Fig. 4. Voltage readings were taken at 5 mm divisions on both sides of a crack cut at 45^o to the specimen surface for 1mm increments of crack growth. The voltage profile of the crack revealed that a skew crack could be readily detected.

The Phase III system was used to analyse the effect on the measured PD of skew cracks at different angles in steel specimens. The voltage profiles for saw cuts were investigated at 1mm crack increments, while the probe was placed over the crack, initially with the crack positioned in the centre of the probes, then with one of the probes 1mm from the crack, then followed by all subsequent measurements taken at 5mm divisions. This facilitated thorough investigation of the voltage profile due to the skew crack. Figure 5 depicts the results obtained by a crack propagated at 45^o to the surface of the specimen.

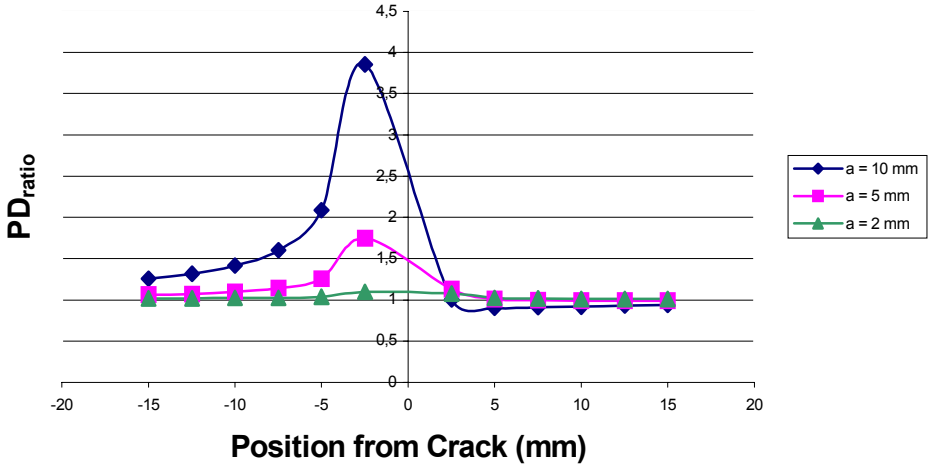

Figure 4. Graph of PD_{ratio} vs Position for a skew crack propagated at 45 degrees to the left, for crack lengths of 2, 5 and 10mm for Phase I.

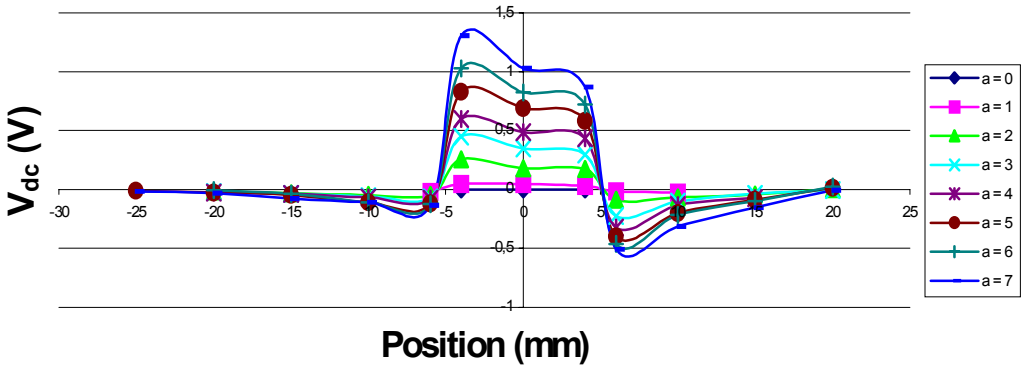

Figure 5. Graph of V_{dc} vs Position for a crack orientated at 45 degrees to the left, for a crack length from 0 to 7mm for Phase III.

The voltage profile is visibly asymmetric, which lends this system to the detection of crack orientation. Figure 6 depicts the difference in voltage between the potential across the crack on the surface, with the crack at the centre of the probes, and with the probe 1mm from the crack on the cracked side of the specimen. This graph displays the different effects that cracks of different orientations have on the measured potential.

As is evident from the results using the present system, the orientation of a crack less than 4mm deep cannot be accurately detected, but the comparison of the measured voltages for a crack greater than 5mm can be used to reveal the orientation of the crack.

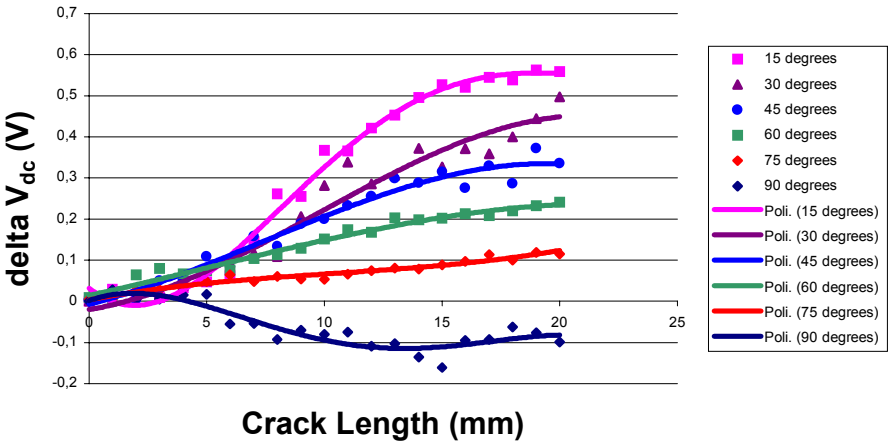

Figure 6. Graph of V_{dc} vs Crack Length for the cracked side of the specimens with crack orientations of 15, 30, 45, 60, 75 and 90 degrees.

Crack Shape Effects

Thumbnail fatigue cracks of two different aspect ratios were grown in the TRB specimens. The potential was measured at 2mm divisions over the length of the crack on the surface to provide a profile of the shape of the crack, as shown in Fig. 7. The voltage profile correlated with the shape of the crack, although the correlation with increasing crack length does not appear to be a linear function. This was due to edge effects of the specimen, as the current was forced to flow in a decreasing area between the crack and the edge of the specimen.

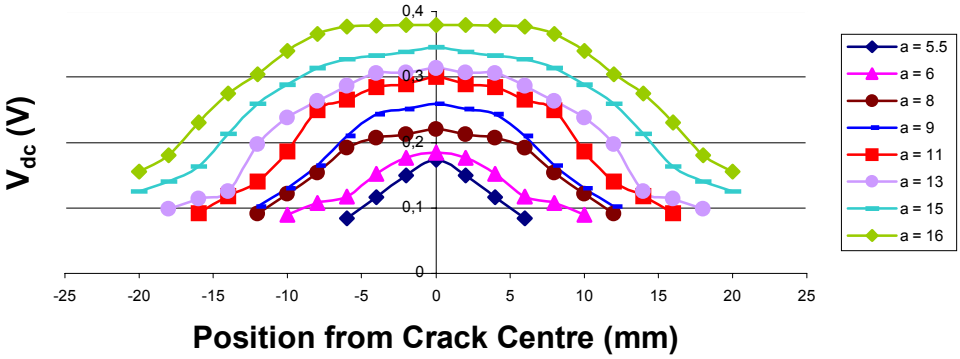

Figure 7(a). Graph of V_{dc} vs Position from the Centre of a thumbnail crack (aspect ratio of 0.253) for different crack lengths.

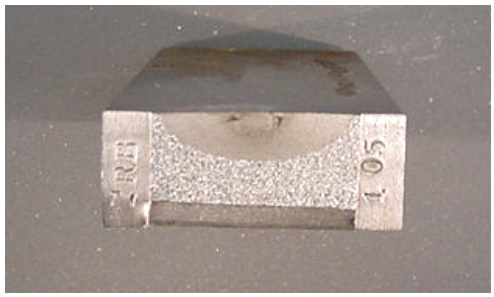

Figure 7 (b). Photograph displaying the actual shape of a thumbnail crack investigated.

Load Effects

Any effect of applied stress across the fatigue crack on the NDT detection system, which could affect the NDT sizing capability, needed to be evaluated. In the present case, for a fatigue cracked sample, the ACPD response as a function of bending load was monitored, for both loading and unloading. There was some small closure effects as the crack opened, presumably due to breaking of previous conduction across crack asperities. Subsequently, the PD curiously dropped with increasing bending stress, which effect may be attributable to magneto-striction effects (5,9, 13,18), as the phenomenon did not occur in similar aluminium samples. In any case, for all practical load cases the error was small (of the order of 50mV) which correlates with an error in flaw sizing of approximately 0.4mm. This was regarded as still acceptable from a practical point of view.

CONCLUDING REMARKS

An ACPD system has been developed for use as an NDT device for evaluating and sizing fatigue cracking in metallic components. In particular fatigue cracking, being sharp and tight, truly represents flaws found in industrial components. The present ACPD system has many advantages over other crack sizing systems, such as remarkably accurate fatigue flaw sizing, to approximately 40 microns, and the ability to distinguish skew cracks and cracks of variable aspect ratio. In addition, the use of a mains power source makes this system extremely practical. This was achieved by the design of an electronic circuit containing the minimum amount of analog components to process the ACPD signals and to reduce inherent errors. The use of a dual probe voltage measurement system further decreased the effects of any electrical noise introduced into the system, and resulted in no significant voltage being induced in the voltage probe leads. The results also suggested that crack closure effects affect the measured potential across the crack, and that the potential also decreases with load in ferromagnetic specimens. Both of these effects are small, however,

when compared with the potential caused by crack extension, but deserve further investigation. The voltage profiles measured on either side of and along the length of the crack revealed that the discrimination of crack orientation and crack profile are both feasible. Thus, the present ACPD system is seen as a precursor in the development of a device, which can be used as a second-tier NDE tool for accurate fatigue crack characterisation.

REFERENCES

1. Smith, R.L. (1968) *Nondestructive testing*, 187-191.
2. Silk, M.G. (1989) *Metals and Materials*, 192-196.
3. Lilley, J.R. and Perrie, C.D. (1997) Developments in NDT, AEA Technology.
4. Lamy, C.A., Rebello, J.M.A., Sauer, A. and Carlier, J. (1996) *Insight* **40**, 421-428.
5. Verpoest, I., Aernoudt, E., Deruyttere, A. and Neyrinck, M. (1980) *Fatigue of Engineering Materials and Structures* **3**, 203-217.
6. Nakai, Y. and Wei, R.P. (1989) *Engineering Fracture Mechanics* **32**, 581-589.
7. Gibson, G.P. (1989) *Engineering Fracture Mechanics* **32**, 387-401.
8. Venkatasubramanian, T.V. and Unvala, B.A. (1984) *Journal of Physics E: Sci. Instrum.* **17**, 765-771.
9. Joyce, J.A. and Schneider, C.S. (1988) *Journal of Testing and Evaluation* **16**, 257-270.
10. Hwang, I.S. and Ballinger, R.G. (1992) *Meas. Sci. Technol.* **3**, 62-74.
11. Soh, A.K. and Bian, L.C. (2001) *International Journal of Fatigue* **23**, 427-439.
12. Green, D.A., Kendall, J.M. and Knott, J.F. (1988) *International Journal of Fracture* **37**, R3-R12.
13. Lee, J.H., Saka, M. and Abe, H. (1997) *Experimental Mechanics* **37**, 32 – 136.
14. Zhou, J. and Lewis, J.M. (1993) *Journal of Physics D: Applied Physics* **26**, 1817-1823.
15. Cost, H., Deutsch, V., Ettel, P. and Platte-Wuppertal, M. (1996) *NDTnet* **1.**
16. Chen, S. and Nagy, P.B. (1998) *NDT&E International* **31**, 1-10.
17. You, C.P. and Knott, J.F. (1986) *Engineering Fracture Mechanics* **24**, 291-305.
18. Beom, H.G. (1999) *Journal of the Mechanics and Physics of Solids* **47**, 1379-1395.